MICROWAVE AND MILLIMETER WAVE QWITT DIODE OSCILLATOR

V.P. Kesan, A. Mortazawi, D.P. Neikirk, and T. Itoh

Department of Electrical and Computer Engineering
The University of Texas at Austin, Austin, Texas 78712

ABSTRACT

We present dc, microwave, and millimeter wave characteristics of different quantum well injection transit time (QWITT) diodes. Small-signal and large-signal device models are used to provide physical device design parameters to maximize output power density. A peak output power of 1 mW in the frequency range of 5-8 GHz has been obtained from a planar QWITT oscillator. This is the highest output power obtained from any quantum well oscillator at any frequency. This result also represents the first planar circuit implementation of a quantum well oscillator. Millimeter wave oscillations at 28-31 GHz in a full-height waveguide circuit with an output power of 30 μW have been obtained. In addition, we present results on improving device efficiency by optimizing the design of the drift region through the use of a doping spike. By optimizing the doping concentration and width of the doping spike, an increase in efficiency from 2% to 5% is obtained, without compromising on output power at X-band.

INTRODUCTION

Quantum well oscillators have been shown to be capable of generating power at high millimeter wave frequencies [1, 2], and there is great expectation that these devices will serve as a useful local oscillator at frequencies between 100-1000 GHz. However, there is considerable debate over the quantum well device structures that must be used to maximize the output power obtained from these devices.

We have proposed an improved quantum well oscillator, the quantum well injection transit time (QWITT) diode [3], consisting of a double barrier structure coupled with a depletion region which increases the specific negative resistance and impedance of the device so that higher output power can be obtained. We have performed both small- and large-signal analyses [4-6] of the QWITT diode in order to develop a model that relates physical device and material parameters to the rf performance of the device.

This paper presents results of microwave and millimeter wave QWITT diode oscillators in both planar and waveguide resonant circuits.

EXPERIMENT

A schematic diagram of the device structures, A through G, used in this study is shown in Fig. 1. Three structures, A, B, and C, consisting of identical quantum well regions but with three different drift region lengths of 500Å, 1000Å, and 2000Å respectively, doped n-type $5x10^{16}$ cm^{-3}, were examined. In addition, structures D through G contain the same quantum well regions but have drift regions consisting of a 100Å doping spike of varying doping concentrations from $5x10^{17}$ cm^{-3} to $5x10^{16}$ cm^{-3} followed by a 1800Å $5x10^{16}$ cm^{-3} GaAs region. The heterolayers were grown in a Varian GEN II MBE system on n^+, (100) GaAs substrates, silicon doped to $3x10^{18}$ cm^{-3}. Device mesas were defined using conventional photolithography and processing techniques. Pulsed (50% duty cycle) and continuous dc current-voltage characteristics at room temperature were measured.

The devices were mounted in WR-90 (8-12 GHz) and WR-22 (33-50 GHz) waveguides using a micrometer-controlled post and whisker-contacted for microwave and millimeter-wave measurements. In addition, devices were mounted in a planar microstrip oscillator circuit designed using a standard microwave CAD package with the diode impedance predicted from the large-signal analysis [5, 7].

RESULTS AND DISCUSSION

As expected, due to the asymmetric structure of the QWITT diode, the dc I-V characteristics for the two bias directions are very different. In any negative resistance diode the voltage and current difference between peak and valley, ΔV_{pv} and ΔI_{pv}, must be as large as possible to increase the device output power; in a low frequency model output power is directly proportional to $\Delta V_{pv} \cdot \Delta I_{pv}$ [8]. For the QWITT diode, ΔV_{pv} is increased through the use of a drift region, but ΔI_{pv} should remain virtually the same as the intrinsic quantum well. This results in an increase in the total output power that can be obtained from the QWITT diode compared to a bare

CH2725-0/89/0000-0487$01.00 © 1989 IEEE

resonant tunneling diode. The dc characteristics for the three devices are summarized in Table I. We can see that while the variation in peak-to-valley current differences, ΔI_{pv}, for the three devices A, B, and C, is quite small, a large increase in ΔV_{pv} is observed in these devices (Table I). For the QWITT bias mode (forward bias, substrate positive), as the length of the drift region is increased from 500Å to 2000Å, the voltage corresponding to the current peak, V_p, increases from 2.4V to 5.1V, and the voltage difference between peak and valley currents, ΔV_{pv}, also increases from 0.3V to 1.17V. In the QWITT mode the peak current density for the three devices is essentially constant at 2.5-3.0x10^4 A/cm^2.

The microwave and millimeter-wave performance of the various QWITT structures is summarized in Tables II and III. Three rf circuits have been tested: a whisker-contacted diode mounted in either a WR-90 or WR-22 waveguide backed by a sliding short (see Fig. 2), and a X-band planar circuit consisting of a resonant microstrip circuit line together with a dc biasing scheme for the diode (see Fig. 3). The planar circuit was designed with a commercial microwave CAD package using a diode impedance as determined from the large-signal model for the QWITT diode [5].

The output power in both waveguide circuits is a sensitive function of the dc bias and the position of the sliding short. With the microstrip circuit oscillations in the frequency range of 2-8 GHz were detected, with a peak output power of 1 mW from device C. The impedance of the planar oscillator circuit is much lower than the waveguide circuit, and the improvement in output power seen in the planar circuit is probably due to a better match to the low impedance of the device. For the different devices, as the length of the drift region is increased from 500Å to 2000Å, the output power increases dramatically in both waveguide and planar oscillator circuits (Table II).

In devices D through G a doping spike was introduced at the beginning of the drift region to reduce the electric field and thus decrease the dc bias, but yet fully deplete the entire drift region. We can see that in devices F and G the doping concentration in the spike is so high that a large fraction of the drift region is not depleted, causing a reduction in rf output power. Device E which contains a 8x10^{16} cm^{-3} spike is the optimum device since it possesses the highest efficiency (5%) and marginally higher output power (1 mW) at the same frequency (5-8 GHz) compared to device D with the uniformly doped drift region. Millimeter wave oscillations in the frequency range 28-31 GHz were obtained in a waveguide circuit from both devices D and E with 30 μW output power.

No attempt was made to optimize the microwave resonant cavity and improve the output power by using either reduced height waveguide or improving the circuit impedance match in the planar circuit. In addition, the device areas used in this study were not optimized [5], and intentionally kept small to avoid excessive heating and consequent heat sinking problems. However, the dramatic increase in output power obtained in devices B and C compared to device A clearly suggests that, as predicted by previous analyses [4-6], the intrinsic device characteristics have been improved through an appropriate choice of drift region length.

CONCLUSION

We have presented dc, microwave and millimeter wave characteristics of QWITT devices. A peak output power of 1 mW in the frequency range of 5-8 GHz has been obtained from a planar QWITT oscillator. This is the highest output power obtained from any quantum well oscillator at any frequency and is approximately five times higher power and twice the output power density than reported in the literature [9] for a comparable frequency. This result also represents the first planar circuit implementation of a quantum well oscillator. Millimeter wave oscillations at 28-31 GHz in a waveguide circuit with an output power of 30 μW have been obtained. There is considerable room for optimization of both the resonant cavity and physical device parameters to maximize output power. Nonetheless, the performance achieved here suggests that through further improvements in device and circuit design higher power output may be possible. It seems clear that the actual power limitations of quantum well oscillators have not yet been determined, and that through the use of QWITT design principles useful power levels may be achieved at high millimeter wave frequencies.

ACKNOWLEDGEMENTS

This work was supported by the Joint Services Electronics Program under AFOSR F 49620-86-C-0045 and the Texas Advanced Technology Program.

REFERENCES

1. E.R. Brown, W.D. Goodhue, and T.C.L.G. Sollner, "Fundamental oscillations up to 200 GHz in resonant tunneling diodes and new estimates of their maximum oscillation frequency from stationary-state tunneling theory," J. Appl. Phys., 64, pp. 1519-1529, Aug. 1988.

2. H. Gronqvist, A. Rydberg, H. Hjelmgren, H. Zirath, E. Kollberg, J. Soderstrom, T. Andersson, "A millimeter wave quantum well diode oscillator," Proc. of the 18th European Microwave Conference, pp. 370-375, Stockholm, Sweden, Sep. 1988.

3. V.P. Kesan, D.P. Neikirk, B.G. Streetman, and P.A. Blakey, "A new transit time device using quantum well injection," IEEE Elect. Dev. Lett., EDL-8, pp. 129-131, April 1987.

4. V.P. Kesan, D.P. Neikirk, P.A. Blakey, and B.G. Streetman, and T.D. Linton, "Influence of transit time effects on the optimum design and maximum oscillation frequency of quantum well oscillators," IEEE Trans. on Elect. Dev., ED-35, pp. 405-413, April 1988.
5. V.P. Kesan, T.D. Linton, C.M. Maziar, D.P. Neikirk, P.A. Blakey, and B.G. Streetman, "Power-optimized design of quantum well oscillators," 1987 IEEE International Electron Device Meeting Tech. Dig., pp. 62-65, Dec. 6-9, 1987.
6. D.R. Miller, V.P. Kesan, R.L. Rogers, C.M. Maziar, and D.P. Neikirk, "Time Dependent Simulation of the Quantum Well Injection Transit Time Diode," Proc. of the 13th International Conference on Infrared and Millimeter Waves, ed. by R.J. Temkin, pp. 5-6, Dec. 5-9, 1988.
7. A. Mortazawi, V.P. Kesan, D.P. Neikirk, and T. Itoh, "Periodic Monolithic Millimeter-wave Quantum Well Oscillator," Proc. of the 13th International Conference on Infrared and Millimeter Waves, ed. by R.J. Temkin, pp. 47-48, Dec. 5-9, 1988.
8. V.P. Kesan, A.Mortazawi, D.R. Miller, T. Itoh, B.G. Streetman, and D.P. Neikirk, "Microwave frequency operation of quantum-well injection transit time (QWITT) diode," Elect. Lett., 24, pp. 1473-1474, 24 Nov. 1988.
9. E.R. Brown, T.C.L.G. Sollner, W.D. Goodhue, and C.L. Chen, "High-speed resonant-tunneling diodes," Proc. of SPIE Conf. on Quantum Well and Superlattice Physics II, vol. 943, pp. 2-13, 17-18 March, 1988.

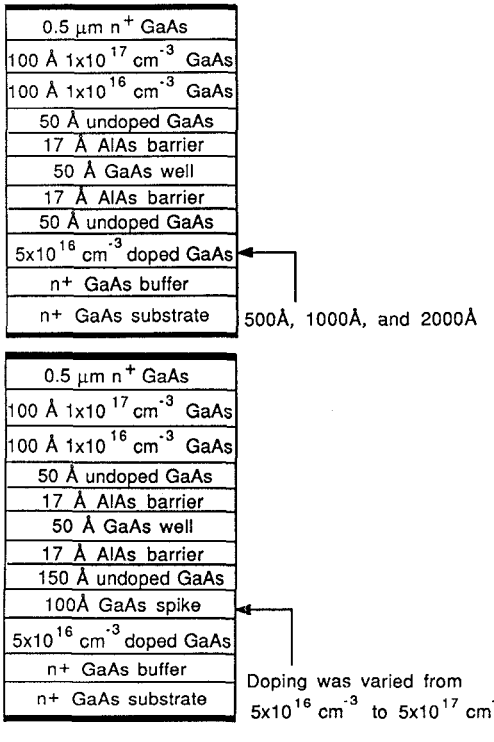

Fig. 1: A schematic cross section of the QWITT diode structures, A through G, examined in this study.

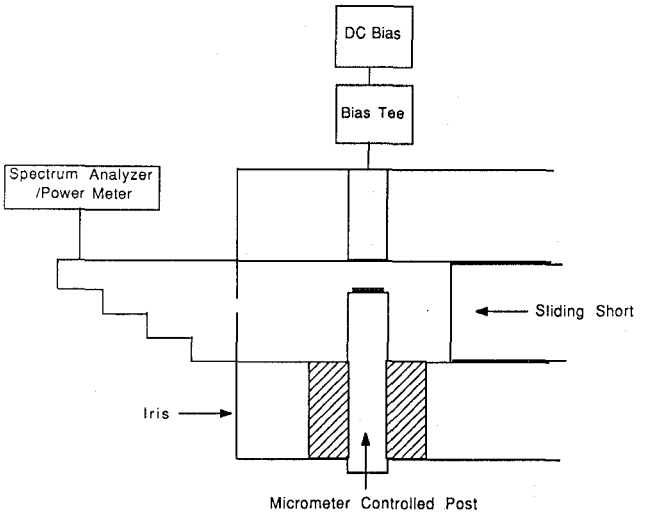

Fig.2: Block diagram of the waveguide circuit used at microwave and millimeter wave frequencies.

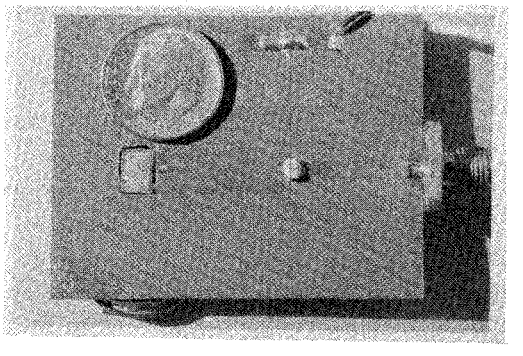

Fig. 3: A planar microstrip QWITT diode oscillator at X-band.

Length of Drift Region (Å)	Drift Region under Accumulation		Drift Region under Depletion		Peak-to-Valley Current Ratio
	Peak Voltage V_p	Voltage Difference between Peak and Valley ΔV_{pv}	Peak Voltage V_p	Voltage Difference between Peak and Valley ΔV_{pv}	
500 (Device A)	1.3±0.1	0.25±0.05	2.42±0.06	0.30±0.08	2.3±0.2
1000 (Device B)	2.95±0.07	0.13±0.05	4.60±0.06	0.51±0.01	1.9±0.16
2000 (Device C)	3.6±0.9	0.08±0.07	5.1±0.14	1.17±0.16	2.1±0.13

Table I: DC characteristics in both bias directions for devices A through C.

Length of Drift Region (Å)	DC Negative Resistance (ohms)	Output Power (μW)	Oscillation Frequency (GHz)
500 (Device A)	64.3±4.8	3 240* 275*	8-12 6-8 6-8
1000 (Device B)	119.2±36.8	10	8-12
2000 (Device C)	378.3±78.0	30 910*	8-12 2-8

* Planar circuit

Table II: Microwave frequency performance of the three QWITT devices, A through C, in both waveguide and planar circuits.

Doping Spike	Output Power (μW)	Efficiency	Oscillation Frequency (GHz)
uniform $5x10^{16}$ (D)	850	3.5%	5 - 8
	13	0.1%	28-31*
$8x10^{16}$ (E)	1000	5.0%	5 - 8
	30	0.1%	28-31*
$1x10^{17}$ (F)	350	4.3%	5 - 8
$5x10^{17}$ (G)	100	3%	5 - 8

* Waveguide circuit

Table III: Microwave and millimeter-wave frequency performance of the QWITT devices, D through G, in both planar microstrip and waveguide circuits.